RSC Advances

This is an *Accepted Manuscript*, which has been through the Royal Society of Chemistry peer review process and has been accepted for publication.

Accepted Manuscripts are published online shortly after acceptance, before technical editing, formatting and proof reading. Using this free service, authors can make their results available to the community, in citable form, before we publish the edited article. This *Accepted Manuscript* will be replaced by the edited, formatted and paginated article as soon as this is available.

You can find more information about *Accepted Manuscripts* in the Information for Authors.

Please note that technical editing may introduce minor changes to the text and/or graphics, which may alter content. The journal's standard Terms & Conditions and the Ethical guidelines still apply. In no event shall the Royal Society of Chemistry be held responsible for any errors or omissions in this *Accepted Manuscript* or any consequences arising from the use of any information it contains.

ROYAL SOCIETY OF CHEMISTRY

www.rsc.org/advances

The interaction of QDs with RAW264.7 cells: nanoparticle quantification, uptake kinetics and immune responses study

O. Gladkovskaya[1,2], V. A. Gerard[3], M. Nosov[4], Y. K. Gun'ko[3], G.M. O'Connor[1], Y. Rochev[2,5*].

1 – School of Physics, National University of Ireland, Galway

2 – Network of Excellence for Functional Biomaterials, Galway

3 – CRANN and School of Chemistry, Trinity College Dublin, Ireland

4 – FarmLab Diagnostics, Emlagh, Elphin, Ireland

5 – School of Chemistry, National University of Ireland, Galway

*Corresponding author: Yury Rochev

email: yury.rochev@nuigalway.ie

phone: (353) 91 492 806

fax: (353) 91 494 596

Conflicts of interests: none declared

RSC Advances Accepted Manuscript

Abstract

Fluorescent semiconductor nanocrystals called quantum dots (QDs) have been proposed as a prominent bio-imaging tool due to their exceptional optical properties. Typically the core size is not greater than 10 nm, thus QDs don't obey models successfully developed and proved on practice for large particles (40-200 nm). This makes difficult to predict the behaviour of such small yet reactive species in physiological media.

Despite the benefits provided by QDs, the challenge of quantifying altered intracellular components remains complicated, and is not clearly investigated, due to interaction of nanoparticles with different cellular compartments. The goal of this work is to investigate uptake kinetics of small green-emitting TGA-capped CdTe QDs with diameter as small as 2.1 nm and to quantify their accumulation inside the cells over the time by flow cytometry. The effect on RAW264.7 monocyte-macrophage cell function and viability also was studied, as monocytes play an important role in innate immunity. The optimal parameters (QD concentration, exposure time, cell activation status) were found; the tested nanoparticles are proven to be applied in short-term assays due to their quick ingestion and accumulation.

Key words: bio-imaging, nanoparticles quantification, quantum dots, monocytes activation, cytotoxicity, flow cytometry

RSC Advances Accepted Manuscript

1. Introduction

Nano-sized particles of well-known bulk materials (such as silica, carbon, titanium dioxide, etc) have enabled many unique possibilities in different technologies and disrupted existing technologies. Engineered nanoparticles are poised to make key impacts in many biological and medical applications, like controllable drug delivery and release systems [1-4], gene diagnostics, and bio-imaging [5]. The question of how these developments can be applied safely in humans remains open. Fluorescent nanocrystals made of semiconductor compounds are called Quantum Dots (QDs). These nanomaterials were first synthesized and named by M. Reed in 1985 [6]. Since that time various uses of QDs have been developed including their applications in photonics, energy harvesting and bio-imaging. Unlike organic fluorochromes, the optical properties of QDs include large Stokes shift, broad absorption and narrow emission, bright fluorescence and high resistance to photobleaching. The set of unique size-tuneable optical characteristics, ease of manufacturing, surface modification and bioconjugation made them eligible alternates for organic dyes as fluorescent agents [7]. However, the discovery of new molecular fluorescent tags and their alternates is under extensive research. For example, steady fluorescent response with good Stokes shift and target mRNA binding has been achieved bio-constructs with perylene-2'-amino-LNA as fluorescence reporter [8]. The vast absorption profile of QDs allows use of a non-specific light source. As shown in Fig. 1, green QDs can be excited by either a violet or a blue laser. In contrast, molecular fluorophores for a maximum efficiency require excitation at a specific wavelength, which is often difficult to achieve because a cytometer is usually fitted with only 2 or 3 lasers. The spectral overlap, which typical for organic dyes limits the number of colours that can be used in single assay; QDs are not limited by this effect.

RSC Advances Accepted Manuscript

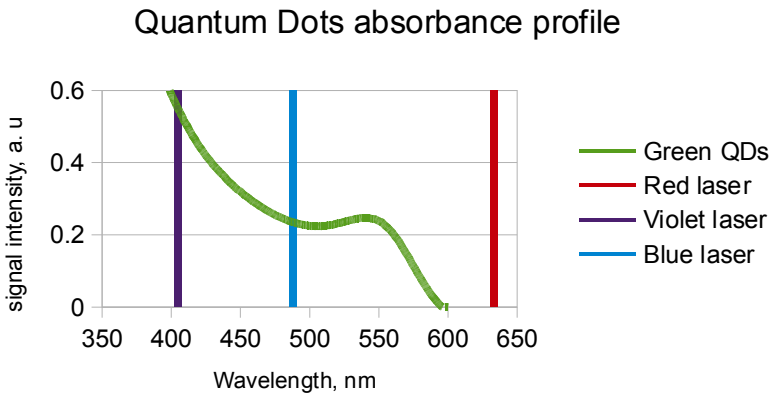

Fig. 1 Possible range of available lasers (vertical lines) and UV-vis absorption of green-emitting QDs used in the study. Due to broad absorption profile QDs don't require excitation on specific wavelength.

Fluorescent proteins (FPs) are great genetic labels which have an option to be in-built into target. Being assembled within a cell, they don't require further fixing/permeabilising or any other cell intervention by exogenous agents. This class of fluorescent tools has been widely explored in live *in vivo* and *in vitro* imaging, and fundamental researches including protein ageing, localisation, morphology etc. The history and application of FPs is excellently described in review by Chudakov [8] and papers by Kremers [9] and Chen [10]. Unless exceptional set of properties provided, FPs have few weak points: 1) large size (25 kDA, whereas molecular fluorophores are just 1 kDA in average) 2) extreme susceptibility to media conditions; even minor pH fluctuations are able to impair FP stability and hence optical properties.

Quantum Dots are shown as prospective fluorescent tags in a range of bio-conjugates, including anti-cancer antibodies, drugs and receptors [11-14]. More details about in vitro and in vivo targeting, delivery and imaging can be found in reviews [15-17]. Molecular Beacons (MBs) technology is a powerful tool in live bio-imaging [18], disease diagnostics and molecular recognition [19,20]. Based on the biochemical principle of selective complementary nucleobases

RSC Advances Accepted Manuscript

binding, MBs enable single-base DNA mismatch detection. It plays a key role in mutations and other pathological alterations detection. Upon binding of complementary sequence, MB opens and thus release a fluorophore. Subsequently, basic hairpin approach has been enormously improved and fitted to different ways of application and recently, such kind of technique is widely implemented in real-time PCR monitoring [21], developing DNA sensors [22], investigations of gene activity [23,24], bio-imaging and cancer targeting [25], DNA-protein interactions [26]. However, the highest FRET response level and signal-to-noise ratio were achieved using semiconductor QDs as fluorescent moiety [19-20]. In our group we have carried out the grafting of molecular beacons to QDs. Obtained hybridized nanoprobes have demonstrated improved optical characteristics, absence of background noise and high affinity to chosen target (data not published).

The inherent function of macrophages is to engulf species recognized as "non-self", such as dead cell debris and bacteria. Macrophage cell response is the first line in adaptive immunity, their surface has a number of markers susceptible to both Toll-like receptors (TLR) and mannose receptors. Another category of surface proteins is responsible for triggering inflammation cascades by expressing inflammatory interleukins (IL), chemokines, cytokines, reactive oxygen species (ROS), nitrite oxide (NO) and cyclooxygenases (COX). Macrophage cells are a convenient *in vitro* model for investigations on QD endocytosis and their further tracking due to quick ingestion within the time scale of live bio-imaging (within a few hours). It can help evaluate all the reactions correctly for objective results to be realised regarding particle efficacy and toxicity.

The main purpose of this work is to describe the uptake kinetics of small nanoparticles (2.1 nm) over the time; also we aimed to develop a simple method for quantum dot intracellular quantification and to investigate QD behaviour at different levels of interaction in physiological media conditions. Particles toxicity, intracellular fluorescence, inflammatory markers expression and cell death mechanism were investigated at 12 and 24 hours time points. Flow cytometry was used to measure cellular responses and quantify nanoparticle ingestion at a specific population

RSC Advances Accepted Manuscript

level.

RSC Advances Accepted Manuscript

2. Materials and methods

2.1 QDs synthesis

CdTe QDs were synthesised according to a previously published procedure [27]. Briefly, Al_2Te_3 reacted with sulphuric acid to produce H_2Te gas which was bubbled through an aqueous solution of $CdCl_2$, thioglycolic acid (TGA) and 0.3g of gelatin, with pH buffered at 11. The molar ratio of Cd:Te:TGA was 1:0.25:1.4. The reaction mixture was then heated under reflux for 2 to 48 hours depending of the desired nanoparticle size. Narrow size distribution fractions were collected via size-selective precipitation using isopropanol.

2.2 UV-vis and PL spectra

Absorbance was examined on a Shimadzu UV-1601 spectrophotometer; distilled water was taken as a baseline. PL spectra were recorded on a Cary Eclipse spectrometer. All measurements were performed to characterize the optical properties of the nanoparticles obtained. More detailed description of as-prepared QDs can be found in the papers previously published by our group [28,29].

2.3 Cell culture

RAW 264.7 murine macrophages cell line was used in this study. Cells were cultured in Dulbecco's Modified Eagle Media (DMEM; Sigma), supplemented with 10% Foetal Bovine Serum (FBS; Sigma), 100 μg/mL of penicillin and 100 μg/mL of streptomycin. Macrophages were maintained in a humidified atmosphere with 5% CO_2 at 37°C.

2.4 Fluorescent microscopy

Cell morphology was tested at each time point. Actin was stained with phalloidin eFluor 760 (eBiosciences) according to recommended procedure. Cells were seeded in density 50,000 per well

RSC Advances Accepted Manuscript

in 4-well chamber slide and let grow overnight. Next day QDs solution was added to the slides and incubated for further 12 or 24 hours. Untreated monocytes were used as control. Afterwards cells were removed from incubator, washed with PBS and fixed with 4% PFA for 15 minutes. Fixed cells were permeabilised with 0.2% TritonX solution for 5 min, washed with PBS and stained with phalloidin for 1 hour. DAPI solution was added to stain nuclei; the slides were viewed immediately under inverted fluorescent microscope.

Live/Dead Assay (Life Technologies) was used to visualize viable and necrotic cells. Cells were treated with QDs as described above. After co-incubation, samples were washed with PBS and stained with calcein and ethidium bromide from the kit as recommended by manufacturer. Slides were proceeded within an hour for fluorescent microscopy.

2.5 double stranded-DNA (ds-DNA) Quantification

Quant-iT Pico Green ds-DNA Assay Kit was used for a precise counting cell number in the probe. The cells were seeded in a 24-well plate to a density of $1x10^5$ cells per well, 24 hours prior to experiment. Different types of QDs (either TGA or TGA-gelatin-covered) within a range of concentrations (1-100 nM final concentration) were added to macrophages. After 24 hours of co-incubation, the cells were progressed to PicoGreen assay according to protocol.

2.6 Annexin V Apoptosis Assay

In this assay cells were seeded to a density of $2.5x10^5$ cells per well in 6 well-plates. After 24 hours of culture, appropriate amounts of QDs were added to each well. Control samples remained untreated. Cells were co-incubated with or without nanoparticles for 12 or 24 hours. Samples were harvested on the day of analysis. Briefly, the reduced media was removed and the cells were washed twice with phosphate buffered saline (PBS). Macrophages were harvested by pipetting in fresh media and then were placed in eppendorf tubes. Cells were washed twice with PBS immediately after harvesting, re-suspended in 500 µl buffer and stained with viability dye according to protocol.

RSC Advances Accepted Manuscript

Afterwards cells were washed with serum-containing buffer. Finally, cells were prepared and stained with Annexin V Apoptosis Assay Kit (eBioscience) and directly proceeded to flow cytometry. All measurements were performed on BD FACS Canto A fitted with 2 lasers (blue, 488 nm; red, 633 nm) and 6 available colours. Unstained cells, single-stained samples, and cells treated with QDs only (without further staining) were used as quality controls.

2.7 QDs uptake and CD80/86 surface markers expression

Flow cytometry was used to detect the amount of internalized nanoparticles and to measure the expression of pro-inflammatory receptors caused by exposure to QDs. All measurements were performed on BD FACS Canto A. In this experiment cells were seeded into 6-well plates to a density of $2.5x10^5$ cells per well and left 24 hours to adhere. The next day, macrophages were loaded with QDs within a range of concentrations (1-100 nM final concentration). After 12 hours of treatment (for the CD86 study) and 24 hours (for the CD80 study), the probes were proceeded to the assay according to a standard protocol. Armenian hamster IgG and Rat IgG2a K were used as isotype controls for CD80 and CD86, respectively. All antibodies and isotype controls were purchased from BioLegend. The standard staining protocol recommended by manufacturer was employed. APC (Allophycocyanin) and FITC (Fluorescein Isothiocyanate) channels were used as references for signal detection. FlowJo software was used for interpretation of results.

2.8 PMA activation and CD86 expression study

Phorbol 12-myristate 13-acetate (PMA) was used to activate monocytes as described elsewhere [30,31]. Cell cultures were prepared as described above. Cell culture media was supplemented with 100 ng/ml of PMA and monocytes were conditioned for 6 hours. Afterwards PMA containing media was replaced by QD solution in normal media. The cells were co-incubated with nanoparticles for 12 hours and proceeded CD86 assay as in previous section. Unprimed monocytes, cells treated only with PMA or QDs and isotype stain were used as controls.

RSC Advances Accepted Manuscript

2.9 Quantification of QDs

The amount of ingested nano-crystals was defined by FlowJo software. At least 10,000 events were recorded per tube. Consistent macrophage population was selected from light scatter graph, the level of fluorescence in FITC channel was evaluated from a histogram plot; the geometric mean value was used quantitatively as a statistical parameter. The percentage of population of interest was found from the overlay of two histograms of cells treated with QDs and untreated controls in the reference channel.

3. Results

3.1 PicoGreen Assay

Fig. 2 presents the results of ds-DNA quantification taken at 24 hours co-culture. Only 100 nM concentration significantly reduces the number of viable cells (either due to necrosis or apoptosis). The inert reaction on 1 and 10 nM can be explained by the threshold effect: a certain critical concentration of particles in system should be achieved to trigger ingestion. To prove it, independent flow cytometry measurements were taken to evaluate intracellular amount of QDs.

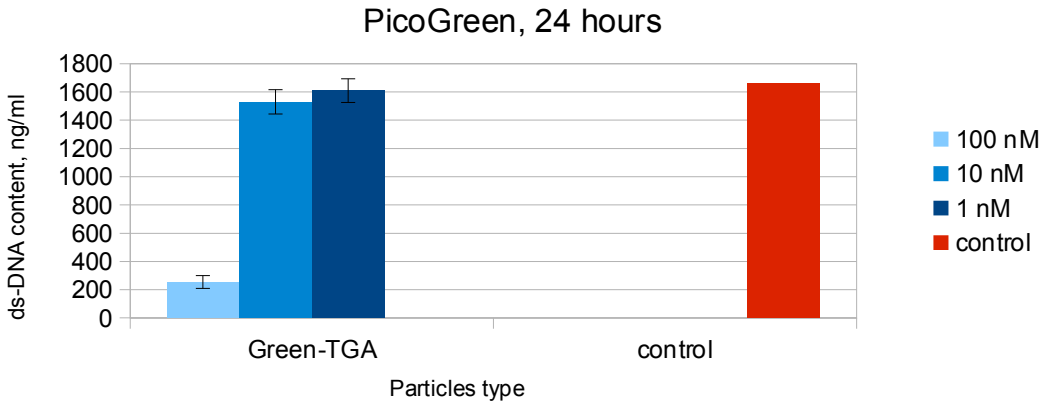

Fig. 2 ds-DNA content in cells introduced to green TGA QDs for 24 hours at various

RSC Advances Accepted Manuscript

concentrations. The low dosage (1 and 10 nM) did not cause any effect in cells. Exposure to high concentration is resulted in significant cell death.

3.2 Cell morphology and Live/Dead assay

Monocytes demonstrate healthy round morphology, actin is uniformly spread compactly around cells without any disruption in samples with QDs concentration less than 100 nM at both time points. Exposure to high concentration of nanoparticles leads to significant reduction cell number. After 24 hours of treatment morphology changes were detected; Fig. 1 in Supplementary Information shows partial nuclei swallowing and necrosis characterised by fracture. Live/Dead assay showed similar results; was confirmed drop in cell number at 100 nM concentration, as well increase in viable/necrotic cell ratio towards necrotic cells (see Fig. 2 in Supplementary Information).

3.3 QDs quantification

The FlowJo software was employed to convert fluorescent emission from cells to relative amount of ingested nanoparticles. Gated consistent cell population with narrow distribution profile was plotted in FITC (green) fluorescence channel. In all samples histograms represented normal distribution.

Signal from cells in the control group (which did not receive any nanoparticles) was taken as baseline. To estimate the percentage of population which ingested quantum dots, histograms of control and treated samples were overlaid. The overlap area was excluded from analysis. Bright sub-population ingested QDs is shifted to the right. By integrating the shifted area can be found the percentage of cells which took up quantum dots.

The intensity of uptake in the reference channel with respect to untreated cells can be semi-quantitatively described. The geometric mean was taken as the signal value; however, other statistic options (median or mean values) are also applicable, due to the fact that the system behaves as a normal distribution.

RSC Advances Accepted Manuscript

3.4 QDs internalizing

Flow cytometry allows accurate collection of fluorescent signal which are quantized for each cell. Cells were grown in presence of QDs for 12 and 24 hours, respectively. Control cultures didn't contain any particles. Comparing flow cytometry data to the results of the PicoGreen study, where no alterations in ds-DNA content in samples treated with the same amount of nanoparticles were observed, it can be concluded that there is no detectable uptake in the case of treatment with concentrations 1-10 nM. Drastic changes were observed for samples exposed to 100 nM. At the 12-hour time point, the tested QDs demonstrated higher fluorescence amplification ratio - compared to

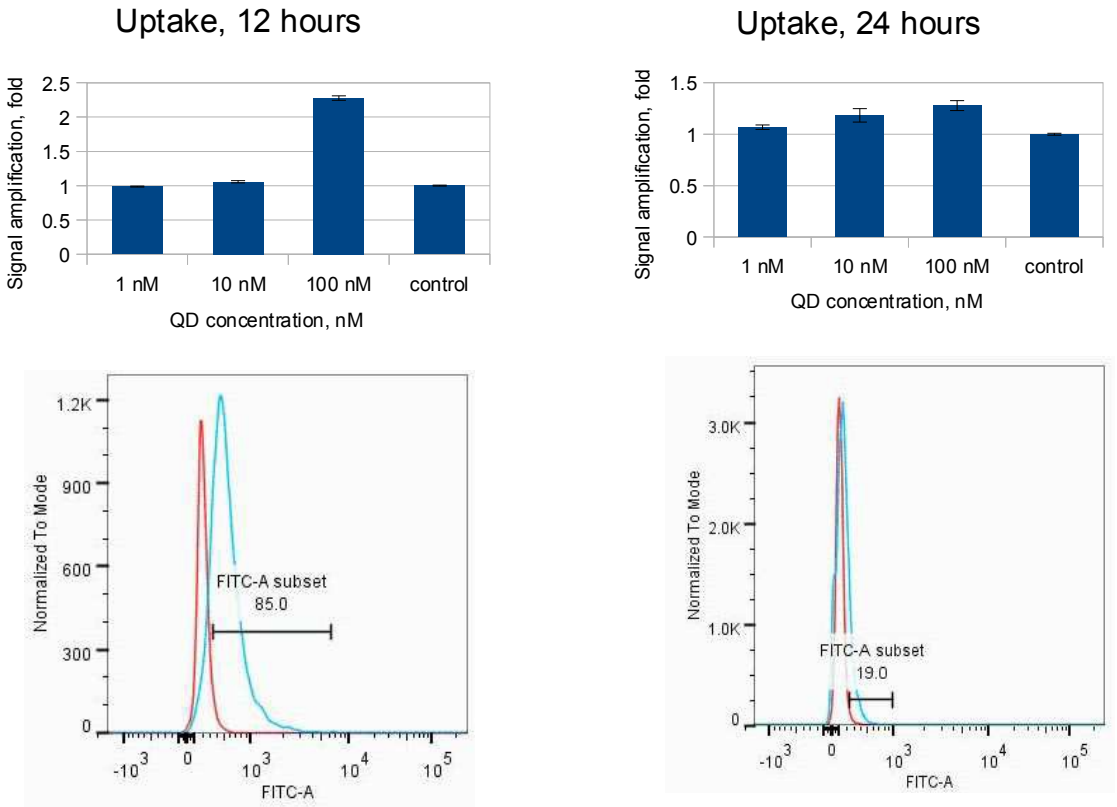

untreated cells. However, 12 hours later there was not much difference among all probes (Fig. 3).

Fig. 3 **A-B:** Green TGA QDs uptake after 12 or 24 hours of co-culture with RAW264.7 cells. The concentration range is 1-100 nM. Similar to PicoGreen, low concentration (1-10 nM) did not affect

RSC Advances Accepted Manuscript

the cells. 2.5-folds fluorescence increase is detected at 12 hours acquisition (A), whereas at 24 hours (B) there's very little difference from control. It can be explained by massive cell death in between 12 and 24 hours and QDs release in cell culture media. **C-D:** Uptake histograms obtained from apoptosis/necrosis assay at 12 (C) and 24 (D) hours tests. X-axis is common logarithm of fluorescent intensity in reference green (FITC) channel. Y-axis is frequency of data distribution. Red line is control (cells did not treated with nanoparticles), blue line is 100 nM treated cells. The overlap area is excluded from uptake count; only cells in area shifted to the right along x-axis are considered in further analysis as containing QDs.

3.5 Apoptosis or Necrosis?

RSC Advances Accepted Manuscript

To answer this question monocytes were cultured for 12 or 24 hours with QDs and subsequently submitted to an Annexin V assay. The Annexin V kit was used to distinguish apoptotic versus necrotic cells stained with fixable viability dye according to protocol. Notable alterations were found in probes treated with 100 nM of QDs. Lower concentrations did not induce any differences compared to control. FITC positive subsets were chosen from histogram overlay of untreated control and 100 nM exposed cells (Fig. 4 C-D). The selected sub-population was divided into 4 quadrants in Annexin V vs. Viability dye channels. Contribution of viable, necrotic, early and late apoptotic cells to uptake was calculated from the mean value of QD fluorescence spectra (FITC). Total uptake was performed as integrated value (number of events in each subset multiplied by mean fluorescence). Fig. 4 represents the resulting signal distribution acquired on 12 and 24 hours

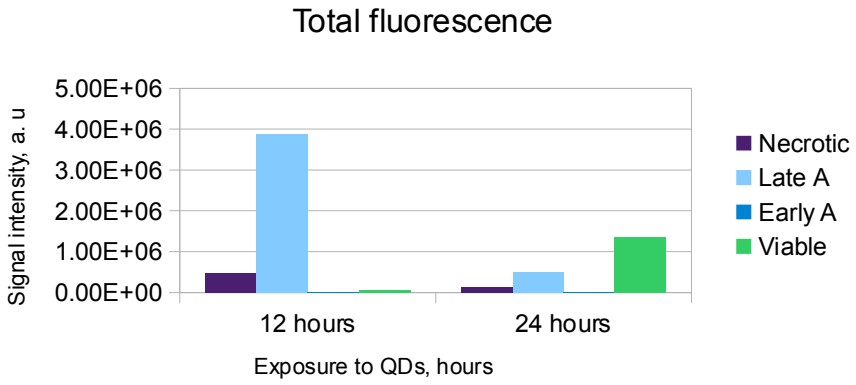

respectively.

Fig. 4 The contribution of each subset in total observed fluorescence from FITC-positive sub-population after 12 or 24 hours of co-incubation RAW264.7 monocytes with 100 nM green TGA QDs. Legend: Necrotic – dead cells followed necrosis pathway, Early A – cells in early apoptosis, Late A – cells in late apoptosis, Viable – live undamaged cells. At 12 hours time point the strongest signal is produced by the cells in late apoptotic stage. At 24 hours signal level is dropped down due to dead cells cleavage and QDs release in the media.

RSC Advances Accepted Manuscript

The general tendency is a small number of early apoptotic cells and a low level of fluorescence from necrotic cells regardless time of exposure. Due to small size and a lack of protective coating, Green TGA nanoparticles were quickly ingested by the cells with significant accumulation (85% positive events) resulted in strong signal. It caused a significant shift to late apoptosis stage (86% of FITC positive sub-population) observed after 12 hours of co-incubation. Late apoptotic subset appears as the main contributor to detected fluorescent signal.

The effects observed after longer time of cell-culture in presence of QDs are determined by intracellular processes triggered by trapping foreign species. Introduction to high concentration of small QDs inevitably led to the degradation of the stabilizing shell and further particle aggregation. Rapidly ingested green TGA-capped QDs caused massive apoptosis and, consequently, cell cleavage. A small percentage of surviving cells showed the less uptake and harvested signal from all QD-treated cells studied here. These observations were confirmed by transmission electron microscopy (TEM) microscopy – significant morphological changes (cytoplasm granulation, chromatin condensation, mitochondria blebbing, presence of QDs in nucleus) were spotted for 100 nM treated probes (see Fig. 3 Supplementary Information); Live/Dead assay demonstrated sudden drop in cell number.

3.6 CD80/86 pro-inflammatory markers expression

Foreign bodies ingested by macrophages can cause inflammatory response as defence reaction. CD80/86 are early pro-inflammatory receptors expressed on RAW264.7 cell surface. These two markers were chosen as convenient indicators to monitor the inflammation process triggered by the QDs. CD80/86 expression was measured simultaneously with particle uptake using flow cytometry. Fig. 5 demonstrates the results of the assays. CD86 expression was acquired after 12 hours of cell treatment with nanoparticles, as this marker is activated earlier than CD80 which was measured at the 24-hour time point. Cells co-incubated with low concentrations of QDs (1-10 nM) demonstrated increased levels of both receptors. It was expected that at 100 nM QD concentration, the level of

RSC Advances Accepted Manuscript

inflammatory markers would be significantly higher due to intensive internalizing and consequent activation of defence mechanism cascades. However the analysed markers were inhibited in this experiment. Fig. 5 depicts observed macrophage behaviour. To investigate on such unexpected effect, cells were activated by PMA followed by QD exposure, the same pattern was detected–

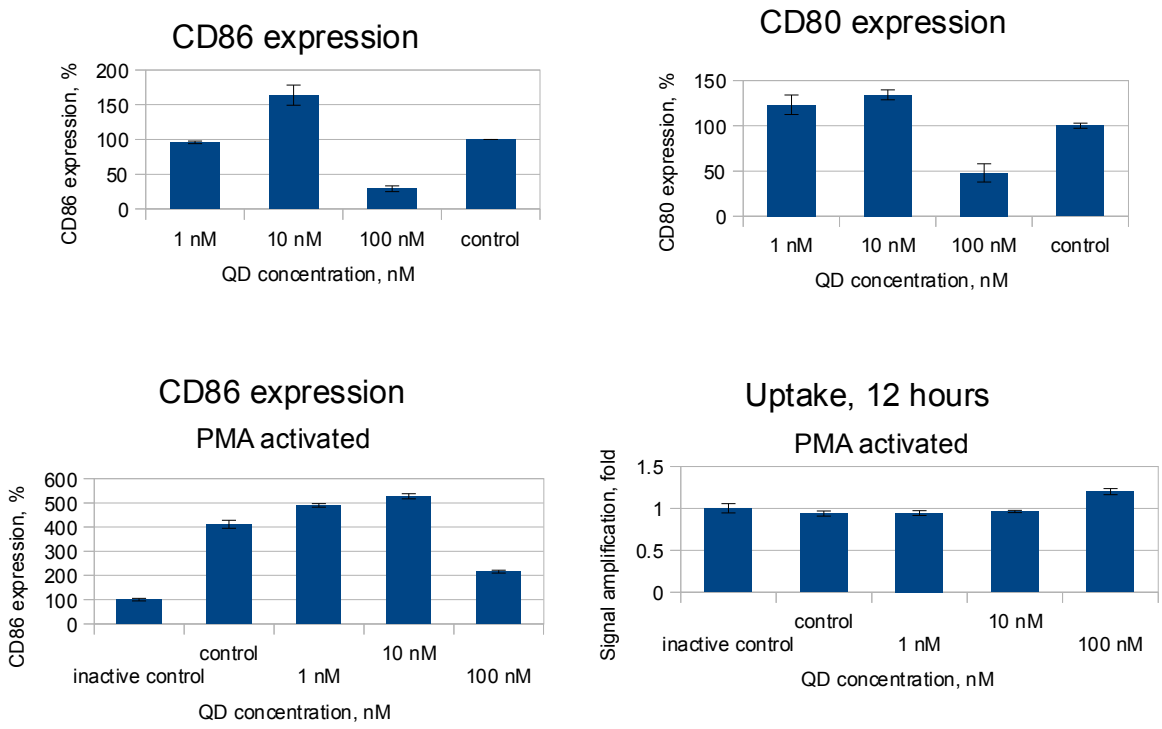

CD86 was suppressed after 12 hours of treatment with nanoparticles.

Fig. 5 **A-B:** CD80/86 expression of unconditioned monocytes at 12 and 24 hours time-points, respectively. Drastic down-regulation of both markers is observed for cells treated with 100 nM QDs. It's related to high number of non-functional (necrotic, late apoptotic) cells and hence their failure to proper expression of the surface molecules. **C:** CD86 expression after preliminary activation of monocytes with PMA for 6 hours. Cells were exposed to green TGA QDs for 12 hours after priming. The activation is confirmed by elevated production of CD86 comparing to unconditioned cells. The same behaviour is observed in non-primed monocytes, where the CD86

RSC Advances Accepted Manuscript

expression is knocked down in 100 nM case. **D:** Uptake pattern for the cells activated by PMA for 6 hours and treated with green TGA QDs for 12 hours.

4. Discussion

Exposure to low doses of QDs (1 and 10 nM) doesn't affect cell function and viability at any time point. Nanoparticles uptake is not linear process, the saturation level has to be achieved to trigger effective ingestion [32]. Highest tested concentration 100 nM had resulted in massive uptake by the cell and number of consequent effects. Fig. 4 shows total intensity of recorded fluorescence and contribution of each cellular subset. It suggests that green TGA QDs due their small size quickly penetrate cells and cause cell damage and death, what we observe after 12 hours of co-incubation. Afterwards, found impaired cells with high amount of QDs are destroyed physically and release nanoparticles back to the media.

The majority of cells take up QDs in first 2 hours (according to Chitrani and Chan's model) [32], followed by their cycle shut down and apoptosis trigger. Early apoptosis is observable after further 2-4 hours of co-culture; as it's quick stage, has not been detected at final 12 hours flow cytometry experiment. Next 4-6 hours late apoptosis is developing, what was observed in experiment. In summary, after 12 hours we have 2 subsets: the small one is without QDs, and the majority one where cells are appeared to ingest nanoparticles, which caused disruption of cell cycle and promoted apoptosis up to late stage. A small amount of live and necrotic cells were also found (1-2%).

In next 12 hours late apoptotic cells are getting eliminating from the system; those survived 1% might undergo 1 division; it gives us a small increase in fluorescent response. We presume that nothing is happening in resistant subset, so it remains neutral to QDs. As result we observe that only 19% of cells have QDs; nearly 60% of this subset are viable and 40% are necrotic. The increase in uptake signal is negligible comparing to 12 hours response.

RSC Advances Accepted Manuscript

It has been shown that nanoparticles uptake depends on number of factors, such as particle size, coating, composition, surface charge, shape, protein corona formation, cytotoxicity, cell type [32-37]. In several works was developed and proved model which states that uptake is happening regardless phase of cell cycle, saturation is achieved once cell underwent full cycle [38,39]. This study was conducted for non-toxic polymer particles (diameter is ≈40 nm). It can be extrapolated to our case, but with certain limitations, as QDs are potent to arrest cell cycle [40-42]. Besides the doubling time, as well as cell type should be take in consideration: macrophages are professional phagocytes which supposed to ingest and destroy foreign body once it's recognised as "non-self". RAW264.7 macrophage-like cell line has been shown as fastest ingesting cell type with high uptake rate [43,44]. Another feature of this cell line is short doubling time – only 11 hours, comparing to HeLa, A549 or U937 cell lines which have 24 hours cell cycle duration.

The prevalent mechanism of nanotoxicity is still under debate. Oxidative stress occurs when cells are treated with nanoparticles and changes mitochondria membrane potential in response. In a classical apoptotic pathway, increased mitochondrial permeability results in cytochrome c release and consequent caspase -9, 3, 6 and 7 cascades activation. The first target is damaged mitochondria itself and ROS generation. Wilhelmi had showed that this mechanism takes place in RAW264.7 cells treated with ZnO nanoparticles [45]. At the same time the results of TEM analysis suggest the hetorogeneity of cell death: necrotic "ghost cells" were also been found as well as apoptotic hallmarks. Moreover, caspase-independent apoptotic route was shown in caspase-9 deficient Jurkat T lymphocytes. The observed cell death mechanisms "combo" has not been related to any particular factors. Same effect – simultaneous presence of apoptosis and necrosis – was studied by M. Liu [46] in A549 lung cancer cells exposed to 10 nm gold nanoparticles. The presence of caspase-independent apoptosis has also been proved by activity of AIF and EndoG proapoptotic factors – triggers of chromatin condensation and DNA shredding. Interestingly, the experiments had different time scale – 6 hours for monocytes and 72 hours for cancer cells, but the same outcome. That's in

RSC Advances Accepted Manuscript

line with the intrinsic cell lines properties – cancer cells are more inert to nanoparticles rather than actively ingesting macrophages [43]. Controversially, Pan et al [47], observing same pattern in HeLa cells treated with 1.4 nm Au nanoparticles, had excluded apoptosis by the fact that zVAD-fmk inhibitor did not prevent cell death hence only necrosis is happening, regardless fact of massive oxidative stress and mitochondria disruption. Caspase 3/7 activity was tested and did not show significant up-regulation in nanoparticle treated cells, but this is the only apoptosis marker has been examined. Basing on later observations of other groups mentioned here [45,46,48] we can speculate that caspase-independent mechanism might have place. Surprisingly, larger (over 60 nm) "non-toxic" silver nanoparticles had continued the trend in causing cell death through both mechanisms [48]. Foldbjerg et all used THP-1 human leukemic monocyte cell line exposed up to 24 hours to Ag nano-crystals and described "typical" picture – high ROS production, fragmented DNA, large amounts of apoptotic and necrotic cells (Annexiv/PI assay). It's hard to say whether co-existence of apoptosis and necrosis has competitive [48] or co-dependent [46] nature. Taken together, our results are in concordance with described above cases, unless QDs are considered as potentially highly toxic agents due to presence of Cd and Te and their small size (2 nm), whereas other studies are dealing with relatively "cell friendly" compounds (Ag, Au, ZnO) and species of similar or greater dimensions. It has to be admitted, that further tests are required to fulfil the knowledge in molecular mechanisms regulating and defying cell fate (apoptosis, necrosis, surveillance) upon the exposure to any nanoparticles, especially to those in a 1-10 nm size range.

It was expected that activity of pro-inflammatory markers CD80/86 will be elevated within the introduced QD concentration. In fact, monocytes did not respond on 1 and 10 nM and got significantly down-regulated when treated with 100 nM. Similar results were observed for other nanoparticles as well, but the source of the phenomenon was not investigated [49-51]. Tsai et al, 2012 [52] attempted to explain inhibition of TLR9 signalling by 4 nm gold NPs in either bone marrow derived primary macrophages and RAW264.7 cell line. They attributed this down-

RSC Advances Accepted Manuscript

regulation to particles with the largest surface-to-volume ratio for NPs ranged up to 45 nm. Hoshino et al, 2009 [53] showed in *in vivo* and *in vitro* experiments that CdSe QDs didn't cause an elevation of anti-bacterial defenders IL-6 and TNF-alpha in peritoneal macrophages, but arrested proliferation of CD4+ T-lymphocytes. It could be related to molecules irresponsiveness to such stimuli as QDs. Thus we carried out another experiment where monocytes were pre-activated by PMA for 6 hours and then treated with QDs for 12 hours. Compared to unconditioned cells, PMA activation had nearly 3 times greater CD86 expression level. The response to low dosage is negligible, whereas 100 nM again arrested CD86 production. We can conclude that the observed disfunction in both cases is consequence of cell damage caused by ingestion of the QDs at 100 nM concentration. Intriguingly uptake pattern for activated monocytes incubated for 12 hours with QDs is the same as for unprimed cells exposed to the same conditions for 24 hours. This is the result that alerted by PMA monocytes are actively ingesting QDs and accelerate cell damage processes. Thus activated monocytes can be used as active cargo to deliver nanoparticles to target cell or inflamed sites.

5. Conclusion

Flow cytometry was explored for quantification of intracellular QDs. Three different concentrations of QDs (1, 10 and 100 nM) were introduced to cell cultures. Only the highest one – 100 nM – was found effective with regards to uptake. We propose that lower concentrations were unable to form vesicles suitable for ingestion, as it was shown by Chithrani and Chan, 2007 [32]. Due to complexity of interaction between QDs and cell culture proteins, surface receptors and cellular organelles, the estimated number of nanoparticles we added to cells is not the same as that detected after certain time of co-incubation. In other words, the initial particles and QDs inside the cells are different species. The advantage of flow cytometry is that it offers a quick measurement of the fluorescent signal from a large number of cells which in turn provides a comprehensive outlook on population level. It helps to evaluate amount of particles taken up without bias. This is important as

RSC Advances Accepted Manuscript

in final distribution one can find some cells either with low and high fluorescence, whereas geometric mean value is a more accurate representation of population.

The exposure to nanoparticles caused unexpected immune responses: we believed that the expression of pro-inflammatory surface markers (CD80/86) would be upregulated in dose-dependent manner. In fact neither 1 nor 10 nM QDs affected the aforementioned parameters. In the case of 100 nM concentration, both receptors were drastically reduced (less than 50% of control). Given the Annexin V assay results this change is not controversial as the majority of cells with high amount of ingested QDs are apoptotic.

The obtained results address few questions to future investigation. First of all, to evaluate the accuracy of flow cytometry, mass spectrometry should be carried out to make a clear correlation between intracellular cadmium content and observed fluorescence. It will also help to understand how QD fluorescent signal changes after interaction with cellular compartments. Further, it's always an open question how much cell line results can be extrapolated on primary cells; next step will be measurement same parameters in primary cultures, particularly antigen presenting cells (e.g. monocytes/macrophages, dendritic cells). It should include an investigation on mechanism behind cell activation and signalling molecules expression upon QD uptake and exposure.

Acknowledgments

This work was conducted under the framework of INSPIRE, the Irish Government's Programme for Research in Third Level Institutions Cycle 5, National Development Plan 2007-2013 with the assistance of the European Regional Development Fund and the Ministry of Education and Science of the Russian Federation (Grant No. 14.B25.31.0002). Authors are grateful to Shirley Hanley (PhD, NCBES) for help with flow cytometry experiments and Pierce Lalor (Anatomy Department, NUIG) for support with TEM processing and imaging.

References

RSC Advances Accepted Manuscript

1 Mitra R. N., Doshi M., Zhang X., Tyus J. C., Bengtsson N., Fletcher S., Page B. D.G., Turkson J., Gesquiere A. J., Gunning P. T., Walte G. A., Santra S. An activatable multimodal/multifunctional nanoprobe for direct imaging of intracellular drug delivery. Biomaterials 2012 (33) 1500-1508. doi:10.1016/j.biomaterials.2011.10.068.

2 Chakravarthy K. V. , Davidson B. A., Helinski J. D., Ding H., Law W-C., Yong K. T., Prasad P. N., Knight P. R. Doxorubicin-conjugated quantum dots to target alveolar macrophages and inflammation. Nanomedicine: Nanotechnology, Biology, and Medicine 2011(7) 88–96. doi: 10.1016/j.nano.2010.09.001

3 Yuan Q., Hein S., Misra R.D.K. New generation of chitosan-encapsulated ZnO quantum dots loaded with drug: Synthesis, characterization and in vitro drug delivery response. Acta Biomaterialia 2010 (6) 2732–2739. doi:10.1016/j.actbio.2010.01.025

4 Pawar H, Douroumis D., Boateng J. S. Preparation and optimization of PMAA–chitosan–PEG nanoparticles for oral drug delivery. Colloids and Surfaces B: Biointerfaces 90 (2012) 102–108. doi:10.1016/j.colsurfb.2011.10.005

5 Li Z. , Wang K., Tan W., Li J., Fu Z., Ma C., Li H., He X., Liu J. Immunofluorescent labeling of cancer cells with quantum dots synthesized in aqueous solution. Anal. Biochem. 2006 (354) 169–174. doi:10.1016/j.ab.2006.04.029

6 Reed M. A. et al. Spatial quantization in GaAs–AlGaAs multiple quantum dots. J. Vac. Sci. Technol. B 1986 (4) 358. dx.doi.org/10.1116/1.583331

7 Chattopadhyay P. K., Price D. A., Harper T. F., Betts M. R., Yu J., Gostick E., Perfetto S. P., Goepfert P., Koup R. A., De Rosa S. C., Bruchez M. P., Roederer M. Quantum dot semiconductor nanocrystals for immunophenotyping by polychromatic flow cytometry. Nature Medicine 2006;12(8): 972-977. doi:10.1038/nm1371

RSC Advances Accepted Manuscript

8 Chudakov D. M., Matz M. V., Lukyanov S., Lukyanov K. A. Fluorescent proteins and their applications in imaging living cells and tissues. Physiol Rev 90: 1103–1163, 2010. doi:10.1152/physrev.00038.2009.

9 Kremers G-J, Gilbert S. G., Cranfill P. J, Davidsonand M. W., Piston D. W. Fluorescent proteins at a glance. Journal of Cell Science 124, 2676, 157-160. doi:10.1242/jcs.095059

10 Chen T-W., Wardill T. J., Sun Y., Pulver S. R., Renninger S. L., Baohan A., Schreiter E. R., Kerr R. A., Orger M. B., Jayaraman V., Looger L.L.,Svoboda K., S. Kim D. S. Ultra-sensitive fluorescent proteins for imaging neuronal activity. Nature. 2013 July 18; 499(7458): 295–300. doi:10.1038/nature12354

11 Tada H.,Higuchi H., Wanatabe T. M., Ohuchi N. In vivo real-time tracking of single quantum dots conjugated with monoclonal anti-her2 antibody in tumors of mice. Cancer Research 2007;67:1138-1144. doi:10.1158/0008-5472.CAN-06-1185

12 Gao X., Cui Y., Levenson R. M., Chung W.K.L., Nie S. In vivo cancer targeting and imaging with semiconductor quantum dots. Nature Biotechnology V. 22, N. 8, August 2004, 969-976 doi:10.1038/nbt994

13 Pan J, Feng S-S. Targeting and imaging cancer cells by Folate-decorated, quantum dots (QDs)-loaded nanoparticles of biodegradable polymers. Biomaterials 30 (2009) 1176–1183. doi:10.1016/j.biomaterials.2008.10.039

14 Savla R.,Taratula O., Garbuzenko O., Minko T. Tumor targeted quantum dot-mucin 1 aptamer-doxorubicin conjugate for imaging and treatment of cancer. Journal of Controlled Release 153 (2011) 16–22. doi:10.1016/j.jconrel.2011.02.015

15 Medintz I. L., Uyeda H. T., Goldman E. R., Mattoussi H. Quantum dot bioconjugates for imaging, labelling and sensing. Nature Materials V. 4 June 2005 436-446. doi:10.1038/nmat1390

16 Biju V., Mundayoor S., Omkumar R. V, Anas A., Ishikawa M. Bioconjugated quantum dots for cancer research: Present status, prospects and remaining issues. Biotechnology Advances 28 (2010)

RSC Advances Accepted Manuscript

199–213. doi:10.1016/j.biotechadv.2009.11.007

17 Smith A. M., Duan H., Mohs A. M., Nie S. Bioconjugated quantum dots for in vivo molecular and cellular imaging. Advanced Drug Delivery Reviews 60 (2008) 1226–1240. doi:10.1016/j.addr.2008.03.015

18 Alexander J., Pandit A., Bao G., Connolly D. and Rochev Y. Monitoring mRNA in living cells in a 3D in vitro model using TAT- peptide linked molecular beacons. Lab Chip, 2011, 11, 3908–3914. doi:10.1039/C1LC20447E

19 Wu S.-M. et al: Direct fluorescence in situ hybridization (FISH) in Escherichia coli with a target-specific quantum dot-based molecular beacon. Biosensors and Bioelectronics 26 (2010) 491–496. doi:10.1016/j.bios.2010.07.067

20 Cady N. C., Strickland A. D., Batt C. A. Optimized linkage and quenching strategies for quantum dot molecular beacons. Molecular and Cellular Probes 21 (2007) 116–124. doi:10.1016/j.mcp.2006.09.001

21 Yeo A. C., Chan K. P., Kumarasinghe G.,Yap H. K. Rapid detection of codon 460 mutations in the UL97 gene of ganciclovir-resistant cytomegalovirus clinical isolates by real-time PCR using molecular beacons. Molecular and Cellular Probes 19 (2005) 389–393. doi:10.1016/j.mcp.2005.06.008

22 Liu X., Farmerie W.,Schuster S., Tan W.Molecular Beacons for DNA Biosensors with Micrometer to Submicrometer Dimensions. Analytical Biochemistry 283, 56 – 63 (2000) doi:10.1006/abio.2000.4656

23 Kihara T., Yoshida N., Kitagawa T., Nakamura C., Nakamura N., Miyake J.Development of a novel method to detect intrinsic mRNA in a living cell by using a molecular beacon-immobilized nanoneedle. Biosensors and Bioelectronics 26 (2010) 1449–1454. doi:10.1016/j.bios.2010.07.079

24 Riches L. C., Lynch A. M., Gooderham N. J.A molecular beacon approach to detecting RAD52 expression in response to DNA damage in human cells. Toxicology in Vitro 24 (2010) 652–660.

RSC Advances Accepted Manuscript

doi:10.1016/j.tiv.2009.09.019

25 Kim J. K., Choi K-J., Lee M., Jo M, Kim S. Molecular imaging of a cancer-targeting theragnostics probe using a nucleolin aptamer- and microRNA-221 molecular beacon-conjugated nanoparticle. Biomaterials 33 (2012) 207-217.doi:10.1016/j.biomaterials.2011.09.023

26 Vitko J., Rujan J., Androga L., Mukerji I., Bolton P. H. Molecular Beacon-Equilibrium Cyclization Detection of DNA-Protein Complexes. Biophysical Journal V. 93 November 2007 3210–3217. doi: 10.1529/biophysj.106.097642.

27 Byrne S. J., Williams Y., Davies A., Corr S. A., Rakovich A., Gunko Y. K., Rakovich Y. P., J. F. Donegan, Volkov Y. "Jelly Dots": Synthesis and Cytotoxicity Studies of CdTe Quantum Dot–Gelatin Nanocomposites. Small Journal, edited by Wiley-VCH Verlag GmbH & Co. KGaA, Weinheim, 2007 (7) 1152-1156. doi: 10.1002/smll.200700090

28 Gérard V. A., Gun'ko Y. K., Prasad B. R., and Rochev Y. Synthesis of Biocompatible Gelatinated Thioglycolic Acid-Capped CdTe Quantum Dots ("Jelly Dots"). Mikhail Soloviev (ed.), *Nanoparticles in Biology and Medicine: Methods and Protocols*, Methods in Molecular Biology, vol. 906, Springer Science+Business Media, LLC 2012, doi:10.1007/978-1-61779-953-2_21

29 Gérard V. A, Maguire C. M , Bazou D. and Gun'ko Y. K. Folic acid modified gelatine coated quantum dots as potential reagents for in vitro cancer diagnostics. Journal of Nanobiotechnology 2011, 9:50, doi:10.1186/1477-3155-9-50

30 Qiao S., Li W., Tsubouchi R., Haneda M., Murakami K., Takeuchi F., Nisimoto Y., Yoshino M. Rosmarinic acid inhibits the formation of reactive oxygen and nitrogen species in RAW264.7 macrophages. Free Radical Research, September 2005; 39(9): 995–1003. doi: 10.1080/10715760500231836.

31 Gieche J., Mehlhase J., Licht A., Zacke T., Sitte N., Grune T. Protein oxidation and proteolysis in RAW264.7 macrophages: effects of PMA activation. Biochimica et Biophysica Acta 1538 (2001) 321-328. doi:10.1016/S0167-4889(01)00083-0

RSC Advances Accepted Manuscript

32 Chithrani D. B., Chan W. C. Elucidating the mechanism of cellular uptake and removal of protein-coated gold nanoparticles of different sizes and shapes. Nano Letters, 2007; 7(6): 1542-1550. doi: 10.1021/nl070363y

33 Clift M. J. D., Rothen-Rutishauser B., Brown D. M., Duffin R., Donaldson K., Proudfoot L., Guy K., Stone V. The impact of different nanoparticle surface chemistry and size on uptake and toxicity in a murine macrophage cell line. Toxicology and Applied Pharmacology 232 (2008) 418-427. doi:10.1016/j.taap.2008.06.009

34 Chithrani B. D., Ghazani A. A., Chan W. C. W. Determining the Size and Shape Dependence of Gold Nanoparticle Uptake into Mammalian Cells. Nano Letters 2006 Vol. 6, No. 4, 662-668. doi:10.1021/nl052396o

35 Walkey C. D., Olsen J. B., Guo H., Emili A., Chan W. C. W. Nanoparticle Size and Surface Chemistry Determine Serum Protein Adsorption and Macrophage Uptake. J. Am. Chem.Soc. 2012, 134, 2139−2147. doi: 10.1021/ja2084338

36 Tenzer S., Docter D., Kuharev J., Musyanovych A., Fetz V., Hecht R., Schlenk F., Fischer D., Kiouptsi K., Reinhardt C., Landfester K., Schild H., Maskos M., Knauer S. K., Stauber R. H. Rapid formation of plasma protein corona critically affects nanoparticle pathophysiology. Nature Nanotechnology, Vol 8, October 2013, 772-781. doi:10.1038/nnano.2013.181

37 Lovrić J., Bazzi H. S., Cuie Y., Fortin G.R.A., Winnik F. M., Maysinger D. Differences in subcellular distribution and toxicity of green and red emitting CdTe quantum dots. J Mol Med 2005; 83: 377–385. doi:10.1007/s00109-004-0629-x

38 Aberg C., Kim J. A., Salvati A.,. Dawson K. A. Theoretical framework for nanoparticle uptake and accumulation kinetics in dividing cell populations. EPL, 101 (2013) 38007, 1-6. dx.doi.org/10.1209/0295-5075/101/38007

39 Kim J. A., Aberg C., Salvati A., Dawson K. A. Role of cell cycle on the cellular uptake and dilution of nanoparticles in a cell population. Nature Nanotechnology, Vol 7, January 2012, 62-68.

RSC Advances Accepted Manuscript

doi:10.1038/nnano.2011.191

40 Liu Y., Wang P., Wang Y., Zhu Z., Lao F.,. Liu X, Cong W., Chen C., Gao Y., Liu Y. The Influence on Cell Cycle and Cell Division by Various Cadmium-Containing Quantum Dots. Small 2013, 9, No.14, 2440–2451. doi:10.1002/smll.201300861.

41 Chen L., Qu G., Zhang C., Zhang S., He J., Sang N., Liu S. Quantum dots (QDs) restrain human cervical carcinoma HeLa cell proliferation through inhibition of the ROCK-c-Myc signaling. Integr Biol (Camb). 2013 Mar; 5(3):590-596. doi:10.1039/c2ib20269g.

42 Wu J., Li H., Chen Q., Lin X., Liu W., Lin J.-M. Statistical single-cell analysis of cell cycle-dependent quantum dot cytotoxicity and cellular uptake using a microfluidic system. RSC Adv., 2014, 4, 24929–24934. doi: 10.1039/C4RA01665C

43 dos Santos T., Varela J., Lynch I., Salvati A., Dawson K. A. Quantitative assessment of the comparative nanoparticle-uptake efficiency of a range of cell lines. Small, 2011, 7 (23): 3341-3349. dx.doi.org/10.1002/smll.201101076

44 Wilhelm C., Gazeau F., Roger J., Pons J. N., Bacri J.-C. Interaction of Anionic Superparamagnetic Nanoparticles with Cells: Kinetic Analyses of Membrane Adsorption and Subsequent Internalization. Langmuir 2002, 18, 8148-8155. doi: 10.1021/la0257337

45 Wilhelmi V., Fischer U., Weighardt H., Schulze-Osthoff K., Nickel C., Stahlmecke B., Kuhlbusch T. A. J., Scherbart A. M., Esser C., Schins R. P. F., Albrecht C. Zinc Oxide Nanoparticles Induce Necrosis and Apoptosis in Macrophages in a p47phox- and Nrf2-Independent Manner. Plos One 15 June 2013, Vol. 8, 6, E65704. doi:10.1371/journal.pone.0065704

46 Liu M., Gu X., Zhang K., Ding Y., Wei X., Zhang X., Zhao Y. Gold nanoparticles trigger apoptosis and necrosis in lung cancer cells with low intracellular glutathione. Springer, J Nanopart Res (2013) 15:1745. doi: 10.1007/s11051-013-1745-8

47 Pan Y., Leifert A., Ruau D., Neuss S., Bornemann J., Schmid G., Brandau W., Simon U., Jahnen-

RSC Advances Accepted Manuscript

Dechent W. Gold Nanoparticles of Diameter 1.4 nm Trigger Necrosis by Oxidative Stress and Mitochondrial Damage. Small 2009, 5, No. 18, 2067–2076. doi: 10.1002/smll.200900466.

48 Foldbjerg R., Olesen P., Hougaard M., Dang D. A., Hoffmann H. J., Autrup H. PVP-coated silver nanoparticles and silver ions induce reactive oxygen species, apoptosis and necrosis in THP-1 monocytes. Toxicology Letters 190 (2009) 156–162. doi: 10.1016/j.toxlet.2009.07.009.

49 Yen H.-J., Hsu S.-H., Tsai C.-L. Cytotoxicity and immunological Response of gold and silver nanoparticles of different sizes, small 2009; 5(13): 1553–1561. doi: 10.1002/smll.200900126.

50 Choi J., Zhang Q., Reipa V., Wang N. S., Stratmeyer M. E., Hitchins V. M., Goering P. L. Comparison of cytotoxic and inflammatory responses of photoluminescent silicon nanoparticles with silicon micron-sized particles in RAW 264.7 macrophages. J. Appl. Toxicol. 2009; 29: 52–60. doi: 10.1016/j.toxlet.2008.10.012.

51 Oh W.-K. , Kim S., Choi M., Kim C., Jeong Y. S., Cho B.-R., Hahn J.-S., Jang J.: Cellular uptake, cytotoxicity, and innate immune response of silica-titania hollow nanoparticles surface functionality, ACS. Nano, V. 4, No. 9, (2010), 5301:13. doi:10.1021/nn100561e

52 Tsai C. Y., Lu S. L., Hu C. W., et al. Size-dependent attenuation of TLR9 signaling by gold nanoparticles in macrophages. Journal of Immunology 2012;188:68–76.doi: 10.4049/jimmunol.1100344

53 Hoshino A., Hanada S., Manabe N., Nakayama T., Yamamoto K. Immune Response Induced by Fluorescent Nanocrystal Quantum Dots *In Vitro* and *In Vivo.* IEEE Transactions On Nanobioscience, March 2009;8(1): 51-57. doi:10.1109/TNB.2009.2016550

8 Astakhova I. V., Korshun V. A., Jahn K., Kjems J., Wenge J. Perylene Attached to 2′-Amino-LNA: Synthesis, Incorporation into Oligonucleotides, and Remarkable Fluorescence Properties *in Vitro* and in Cell Culture. Bioconjugate Chem. 2008, 19, 1995–2007 1995. doi:10.1021/bc800202v

RSC Advances Accepted Manuscript

Table of Contents graphic

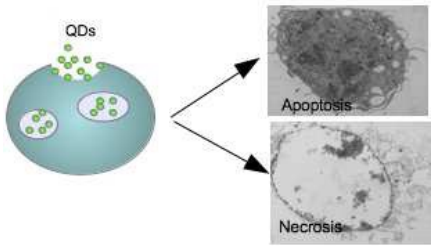

Exposure to small QDs in high concentration in continuos cell culture results in cell death by apoptosis and necrosis co-existing within the same cell population.

RSC Advances Accepted Manuscript